2024 Scienceline Publication

Journal of Civil Engineering and Urbanism

Volume 14, Issue 3S: 229-237; September 15, 2024 **ISSN-2252-0430**

DOI: https://dx.doi.org/10.54203/jceu.2024.24

Flexible Vegetation Behavior under Varying Areal Densities and Effects on Flow Structures: Numerical Observations

Afis O. Busari[1] and Kelvin A. John[2]

[1]*Department of Civil and Mining Engineering, University of Namibia, JEDS Campus, Ongwediva 15006, Namibia*
[2]*Department of Civil Engineering, University of Abuja, Federal Capital Territory, Abuja 00234, Nigeria*

Corresponding author's Email: abusari@unam.na

RESEARCH ARTICLE

PII: S2252043024000024-14

Received: June 25, 2024

Revised: September 02, 2024

Accepted: September 05, 2024

ABSTRACT

This study carried out extensive numerical studies on a refined "One dimensional (1-D) Reynolds Averaging Navier-Stokes (RANS) Model" for vegetated open channel flow. In the 1-D RANS model, the Spalart Allmaras closure model was used to model the turbulence caused by eddies within the vegetation zone and the interface between the top of the vegetation and the clear water zone. In this work, numerical simulations using 1-D RANS model are carried out using dataset obtained from the laboratory under different hydraulic conditions of varying areal vegetation densities. Three classes of highly flexible vegetation densities were simulated: low, medium and highly dense vegetation. The model predictions in terms of mean vertical stream-wise velocity profile and Reynolds Shear Stresses were compared with the laboratory flume experimental results. The 1-D RANS model performances were satisfactory for low and medium densities. However, discrepancies were seen in the model prediction for highly dense vegetation. Hence, the hydraulic roughness parameters in the numerical model has been modified for model re-calibration to capture the position of zero-displacement of velocities. Using the modified parameters, the velocity profiles and the Reynolds Shear Stresses were predicted with very low uncertainty.

Keywords: Zero-displacement parameter, 1-D RANS model, Reynolds shear stresses, areal density, flexible vegetation

INTRODUCTION

The importance of vegetation as a component of aquatic ecosystems cannot be over-emphasized. It has ecological benefits in improving water quality and reducing soil erosion by altering the flow magnitude (Truong and Uijttewaal, 2019; Abdullahi and Busari, 2021). Numerical simulation is an effective approach to show the flow structure in a vegetated channel when the right turbulent modeling is combined with continuity and momentum equations (Li and Busari, 2019; Manko and Busari, 2020).

In-banks vegetation or emergent and submerged floodplain vegetation in rivers and streams have significantly affects the lateral and vertical velocity distributions of flow especially on the turbulence statistics (Chiaradia et al., 2019).

Accurate quantification of the bulk effects of flow-vegetation interaction is a significant challenge in the field of eco-hydraulics as well as of great importance in the design of flood protection or stream restoration schemes (Errico et al., 2019). It has been established that both density and distribution of submerged aquatic weeds had a significant impact on the efficiency and equitability of water distribution (Di Stefano et al., 2022). Thus, increasing the density or distribution of vegetation in a channel, reduces the flow and attenuate the downstream flow and consequently the upstream will be subjected to flooding.

In spite of the above, vegetation has the ability to increase bank stability, reduce erosion and turbidity, provide habitat for aquatic and terrestrial wildlife, attenuate downstream floods, present aesthetic properties and filter pollutants (Ferro and Porto, 2018).

Sequel to the above ecological functions, efforts are now being made at the global level for restoration and rehabilitation of the waterways, flood plain management and restoration of river ecosystems. To understand the impact of vegetation roughness on inducing frictional resistance to flow, more research is needed and to achieve this, both experimental study and numerical simulation are performed considering the effect of vegetal density, plants' flexibility, and channel slope on flow structures by incorporating a zero-displacement parameter to capture the scale of turbulence vis-à-vis the position of zero velocity

near the bed. To this note, the paper presents a 1-D RANS model that includes all essential hydraulic parameters to enhance the accurate prediction of the flow structures in a shallow vegetated watercourse. More so, the study provides an extensive dataset for the validation and subsequent recalibration of the index variables of zero-displacement parameters.

MODEL THEORETICAL BACKGROUND

One dimensional model

In this study a refined 1-D version of the model developed by (Busari and Li, 2006) has been used, in the model, vegetated flows are assumed unidirectional for shallow flow depth. Multi-dimensional models require more laborious and time-consuming for the generation of a large number of synthetic data.

Several experimental cases were simulated using the model. The dataset is obtained from the laboratory experiments which contain nine variables for blade-type vegetation: flow depth (h), Energy slope (S) stem width (B), vegetation height (k_v), vegetal thickness (t), flow rate (Q) flexural rigidity (EI) and number of strips or stems per unit Area (N) and drag coefficient (C_d).

Governing equations

Continuity equations and horizontal momentum equation, represented by (Eqn. 1) and (Eqn. 2) respectively.

$$\frac{\partial u_i}{\partial x_i} = 0 \qquad i = 1 \tag{1}$$

$$\frac{\partial u_i}{\partial t} + u_j \frac{\partial u_i}{\partial x_j} = \frac{\partial}{\partial x_j}\left[\nu_m \left(\frac{\partial u_i}{\partial x_j} + \frac{\partial u_j}{\partial x_i}\right) + \frac{\tau_{ij}}{\rho}\right] - \frac{1}{\rho}\frac{\partial p}{\partial x_i} - \frac{1}{\rho}F_i + g_i \quad I=1, j=3 \tag{2}$$

where x_i $(= x_1)$ = coordinate in horizontal direction *(m)*; u_i $(= u_1)$ = time-averaged velocity in horizontal direction (*m/s*); u_j= 0; t = time (*s*); ρ = fluid density (kg/m^3); ν_m = molecular viscosity (m^2s^{-1}); $\tau_{ij} = -\rho u_i' u_j'$ = Reynolds stresses (N/m^2); p = pressure (N/m^2) is assumed to be a constant; $F_i = F_x$ (N/m^3) is the resistance force components per unit volume induced by vegetation in x directions; g_i is the x-component of the gravitational acceleration and is set to gS_0, where S_0 = channel bottom slope.

The Reynolds stresses are represented by the eddy viscosity model (Eqn. 3):

$$\frac{\tau_{ij}}{\rho} = -\overline{u_i u_j} = -2\nu_t\left(\frac{\partial u_i}{\partial x_j} + \frac{\partial u_j}{\partial x_i}\right) - \frac{2}{3}\delta_{ij}k \quad i=1, j=3 \tag{3}$$

where $k = {}^1/_2\,\overline{u_i' u_i'}$= turbulent kinetic energy (m^2s^{-2}) which can be absorbed into the pressure gradient term and ν_t = eddy viscosity (m^2s^{-1}).

Turbulence closure model

The eddy viscosity ν_t is specified by the Spalart-Allmaras (S-A) turbulence model which involves the solution of a new eddy viscosity variable, ν. The version of the model used is for near-wall region and moderate Reynolds number (Spalart and Allmaras, 1994). The S-A model is intrinsically a transport equation for the eddy viscosity developed under the well-known Boussinesq hypothesis and it is as follows (Eqn. 4):

$$\frac{\partial \nu}{\partial t} + u_j\frac{\partial \nu}{\partial x_j} = C_{b1}\tilde{S}_\nu \nu + \frac{1}{\rho}\left\{\frac{\partial}{\partial x_j}\left[(\nu + \nu_m)\left(\frac{\partial \nu}{\partial x_j}\right)\right] + C_{b2}\left(\frac{\partial \nu}{\partial x_j}\frac{\partial \nu}{\partial x_j}\right)\right\} - C_{w1}f_w\left(\frac{\nu}{d}\right)^2 \tag{4}$$

The eddy viscosity and its magnitude including the constants of the model are well defined in (Spalart and Allmaras, 1994).

The vegetation induced drag force

On the influence of vegetation, the resistance force due to vegetation is defined by the quadratic friction law. The drag force is resulted from wake formation downstream of the stem. The average force per unit volume within the vegetation domain is obtained by (Eqn.5)

$$F_i = Nf_i = \frac{1}{2}\rho C_d NB u_i\sqrt{u_i u_j} = \frac{1}{2}\rho f_{rk} u_i \sqrt{u_j u_j}_{i=1} \tag{5}$$

where N = vegetation density (defined as the number of stems per unit area,$1/\mathrm{m}^2$) and $f_{rk} = C_d NB$.

Flexibility accountability using (Large deflection theory of analysis)

A large deflection analysis based on the Euler-Bernoulli law for bending of a slender transducer has been used to determine the large deflection of the plant stem. The analysis modeled each vegetation stem as a vertical in-extensible non-prismatic slender transducer of length, l. The water flows produce variable distributed loads $q_x(s)$ on the transducer along the x-direction. According to Euler-Bernoulli's law, the local bending moment is proportional to the local curvature.

$$M(s) = EI(s)\frac{\frac{d^2\delta}{ds^2}}{1-\left(\frac{d\delta}{ds}\right)^2} \tag{6}$$

where, M is the bending moment (Nm), s is the local ordinate along the transducer, E is the modulus of elasticity (N/m^2), I is the Second moment of area (m^4) and, δ is the deflection in x-direction (m).

The equilibrium of forces and momentum gives

$$\frac{d^2M}{ds^2} + \frac{dM}{ds}\frac{\frac{d\delta}{ds}\frac{d^2\delta}{ds\,ds^2}}{\left[1-\left(\frac{d\delta}{ds}\right)^2\right]} = -q_x(s)\sqrt{1-\left(\frac{d\delta}{ds}\right)^2} \tag{7}$$

Combining of (Eqns. 6 and 7) yielded a fourth order nonlinear (Eqn. 8) in the deflection δ

$$\frac{d^2}{ds^2}\left[EI(s)\frac{\frac{d^2\delta}{ds^2}}{1-\left(\frac{d\delta}{ds}\right)^2}\right]+\frac{d}{ds}\left[EI(s)\frac{\frac{d^2\delta}{ds^2}}{1-\left(\frac{d\delta}{ds}\right)^2}\right]\frac{\frac{d\delta d^2\delta}{ds\,ds^2}}{\left[1-\left(\frac{d\delta}{ds}\right)^2\right]}=-q_x(s)\sqrt{1-\left(\frac{d\delta}{ds}\right)^2} \quad (8)$$

The vegetation stem is taken as inextensible as the total length remains constant. By dividing the stem into n equal part of constant lengthΔs, the z-ordinate of the i^{th} node is obtained by (Eqn.9)

$$z_i=\sum_{j=1}^{i=n}\sqrt{\Delta s^2-(\delta_i-\delta_{i-1})^2} \quad (9)$$

Numerical methods and boundary conditions

The deflected height of the stem is then equal to z_n. The (Eqn. 9) is then solved using a quasi-linearized central finite difference scheme. To minimize computational effort, the solution can be expressed in non-dimensional form relating the deflected height of vegetation to the applied force, hence, it is approximated by a polynomial.

At the free surface, zero pressure and zero gradients of velocity component are specified:

$$p=0 \quad and \quad \frac{\partial u_i}{\partial \sigma}=0 \quad (10)$$

At the bottom, the logarithmic law wall function is given by (Eqn.11)

$$u=u_w\left[\frac{1}{\kappa}ln\left(\frac{u_w z}{\nu_m}\right)+B\right],\ \nu=\kappa\, z\, u_w \quad (11)$$

where u_w = wall shear velocity (m/s); z = distance from the wall (m); and $B = 8.5$. By knowing the velocity at the point next to the wall with distance, z the wall shear stress can be computed iteratively.

The above equations were coded script using C^{++} language. The bulk drag coefficient is estimated as (Eqn.12):

$$\frac{C_d\lambda k_v}{2B^2h^3}\frac{Q^2}{\left(1-\phi\frac{k_v}{h}\right)^3}-gS=-\left(g-\frac{Q^2}{B^2h^3}\right)\frac{\Delta h}{\Delta x} \quad (12)$$

The solid volume fraction of the vegetation zone is defined by $\phi=NBt=\lambda t$ (-). The frontal area of vegetation per unit volume (areal density) is then given by $\lambda=NB$ (m^{-1}). The Δx, is a small longitudinal distance and Δh is the resulted change in the hydraulic head (water level difference) due to the change. These parameters are captured in the model (Figure 1).

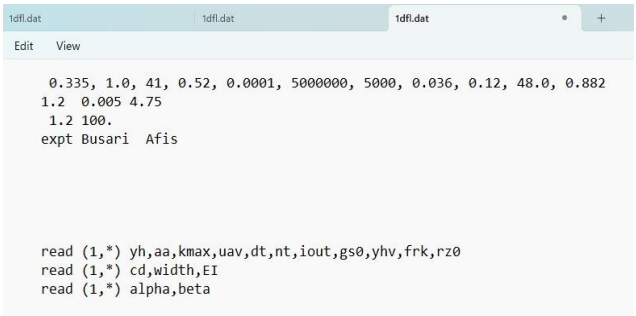

Figure 1. Modelled hydraulic conditions/Input data file

RESULTS AND DISCUSSION

Recently, Azorji and Busari, (2021) and Abdullahi and Busari, (2021) carried out extensive laboratory flume experiments and field investigations on flexible vegetation growth in waterways with varying areal densities. Hence, the need for this study to further validate the 1-D RANS model towards its application to highly dense flexible vegetation under laboratory control experiments and field studies. A screenshot of the simulation time step and stage is shown in Figure 2).

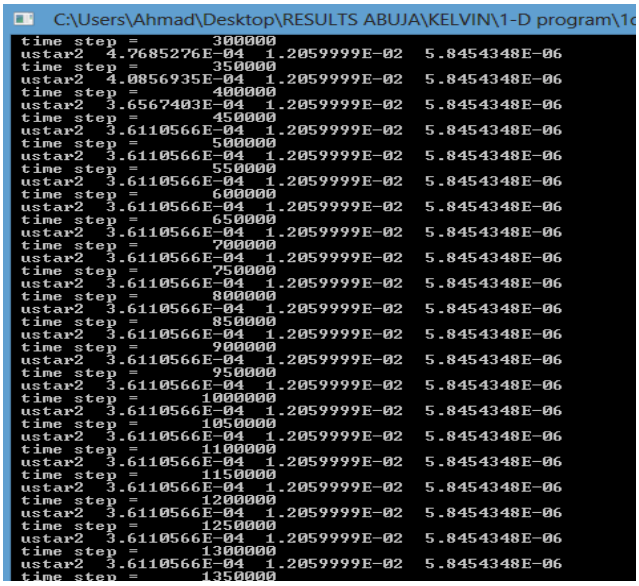

Figure 2. Simulation stage and Time step

General experimental hydraulic conditions

In the studies, Azorji and Busari, (2021) and Abdullahi and Busari, (2021) categorized areal vegetal density into three (3) categories: (i) less dense; (ii) dense vegetation and (iii) high density vegetation. The hydraulic parameters are shown in (Table 1). The details of the flume experiment conducted can be found in (Azorji and Busari, 2021; Abdullahi and Busari, 2021). The maximum discharge throughout the experiment was 50 cm^3/hr.

Table 1. Hydraulic conditions

Author	Hydraulic parameters		Density class
	Vegetation parameter	Flow parameter	
Azorji and Busari, (2021)	$B = 0.0076\ m$; $10 \le N \le 540\ m^{-2}$; $0.3 \le C_d \le 0.7$; $k_v = 0.12m$	$h = 0.35\ m$; $10^{-2} \le$ gS ≤ 0.04	Low
Abdullahi and Busari, (2021)	$B = 0.0022\ m$ $600 \le N \le 3200\ m^{-2}$; $0.6 \le C_d \le 1.2$; $k_v = 0.34\ m$	$h = 0.62\ m$; gS $= 10^{-2}$	Medium
Abdullahi and Busari, (2021)	$B = 0.0022\ m$ $4250 \le N \le 8000\ m^{-2}$; $0.8 \le C_d \le 1.0$; $k_v = 0.34\ m$	$h = 0.62\ m$; gS $= 10^{-2}$	High

Modeling of low vegetal density

Vertical mean stream-wise velocity profile

The result in Figure 3 clearly indicates the influence of vegetation density on the velocity profile in a vegetated canopy. On both axes, the variables are normalized. The shear velocity ($u^* = \sqrt{gS\ (h - k_v)}$ on the horizontal axis to yield scaling parameters.

The entire shape of low density vegetation (e.g.$10 \leq N \leq 90m^{-2}$) from the depth of zero-displacement within the vegetation zone through the clear water zone follows an exponential law. The trend changes as the density increases. For $90 \leq N \leq 210\ m^{-2}$, a point of inflexion is observed slightly at the interface between the deflected vegetation height (see the green dotted line) and clear water zone. Hence, the shape of the velocity profile above the vegetation zone begins to change from exponential to logarithmic law, whereas the nature of the velocity profile within the vegetation zone remains exponential. Beyond, *N=210*, the profile is defined as S-shape. It can be observed that the RANS model predicted all the shape and profile transformations as observed in the laboratory experiment.

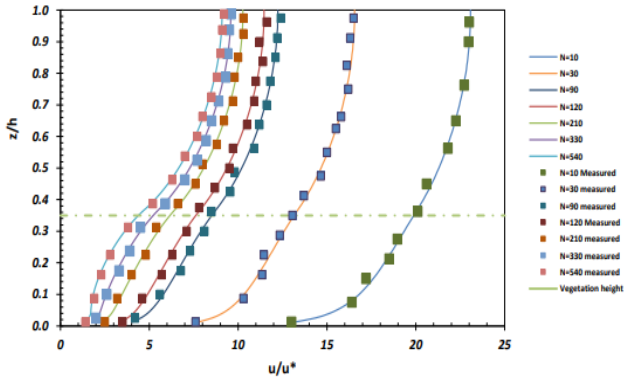

Figure 3. Mean vertical stream-wise velocity profile for flexible, less dense areal vegetation

Reynolds shear stresses in a low density vegetated channel flow

The Figure 4 shows the predictive power of the 1-D RANS model to replicate the measured Reynolds shear stresses $(-/uw/)$**.** The values of the max shear stresses at the interface between the top of the vegetation and the clear water zone are highly correlated with the laboratory observed values for the varying areal densities. The results show the instability of the shear stresses just above channel bed due induced vegetation drag by the flow hydraulic resistance from the vegetation.

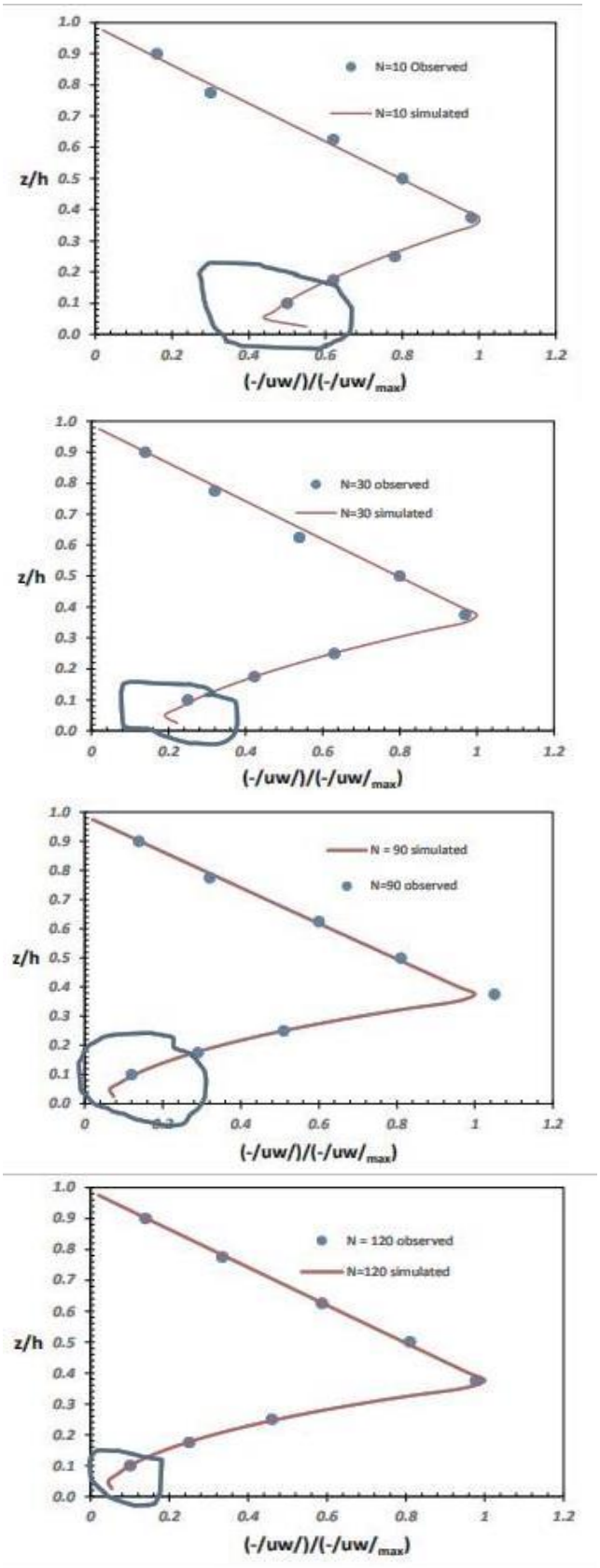

Figure 4. Measured and modelled longitudinal Reynolds shear stresses (low vegetal density).

Modeling of medium vegetal density

Vertical mean stream-wise velocity profile

Figure 5 shows that the experimentally predicted S-shaped vertical mean stream-wise velocity profile was perfectly replicated by the RANS model. The replication is very good from the measured point above the channel bed up to the water surface. It apparent that the points of inflexion are entirely below the deflected heights (the horizontal dotted line) of the vegetation. The location of point of the inflexion rises towards the vegetation height with increasing vegetal density due to the reduction in the vortex shedding at the interface between the vegetation zone and the clear water zone.

Reynolds shear stresses in a medium dense vegetated channel flow

In Figure 6, a good correlation exists between the experimental and modelled results. The prediction was perfect up to the position of the least shear stresses. The scale of the vortex produced became minimal as the vegetation resistance balanced the gravitational flow forces.

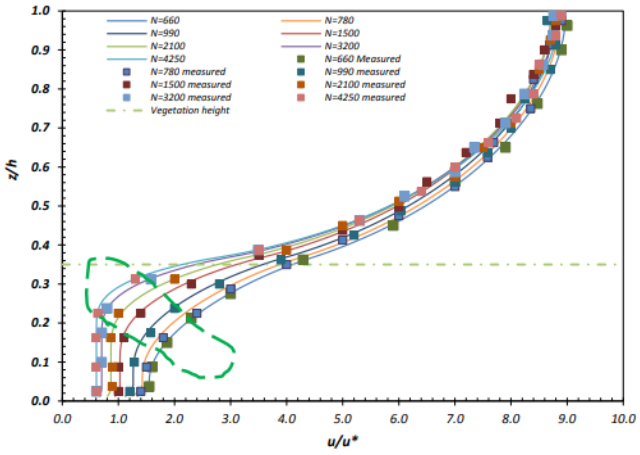

Figure 5. Mean vertical stream-wise velocity profile for flexible, medium dense areal vegetation

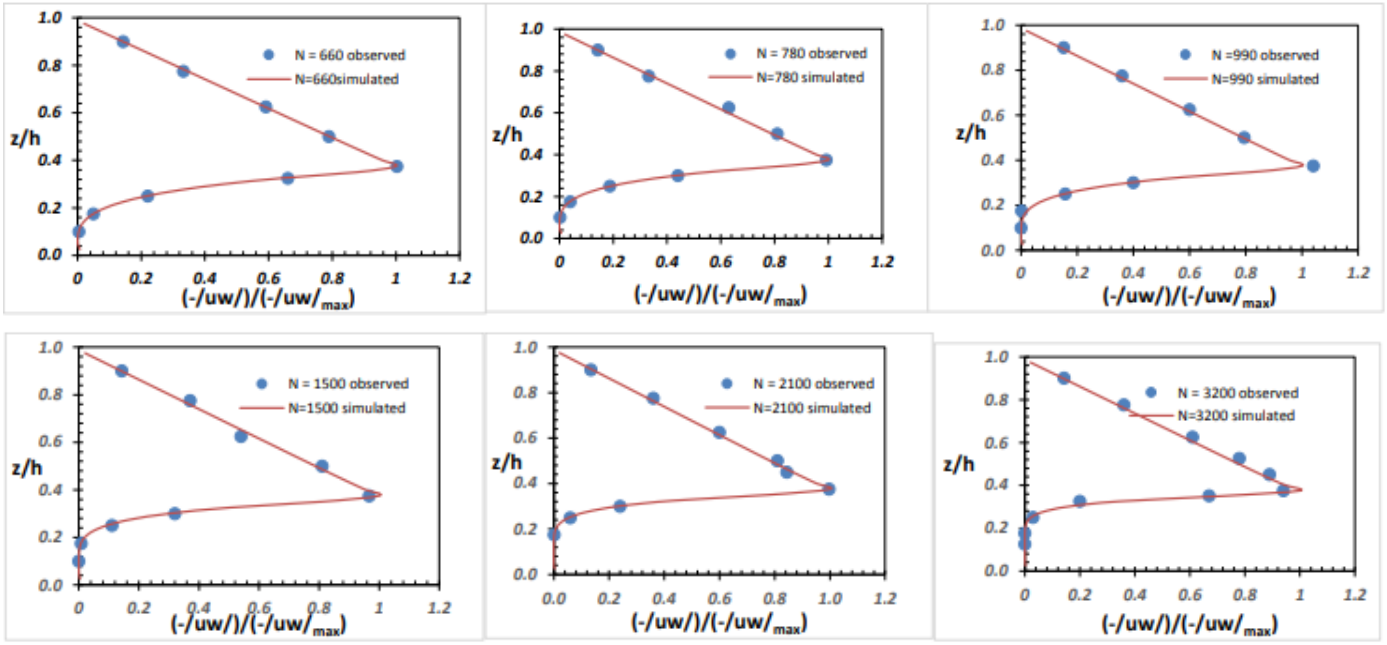

Figure 6. Measured and simulated Reynolds Shear Stresses (medium density vegetation)

Modeling of highly dense vegetal cover

Vertical mean stream-wise velocity profile

Figure 7 shows the model prediction of velocity profile against the experimental results. The RANS model under-predicted the velocities with the vegetation zone for the range vegetal densities and the reduced turbulent scale becomes difficult to replicate. Its predictive capability decreases for $N = 7000$ and 8000 due to over-estimation of the mean velocity close to the water surface. This variation could be attributed to the secondary current produced at the interface between the boundary wall and flowing water. To account for this deficiency in the model prediction, the roughness parameters in the zero-displacement equation used in the model need to be re-calibrated.

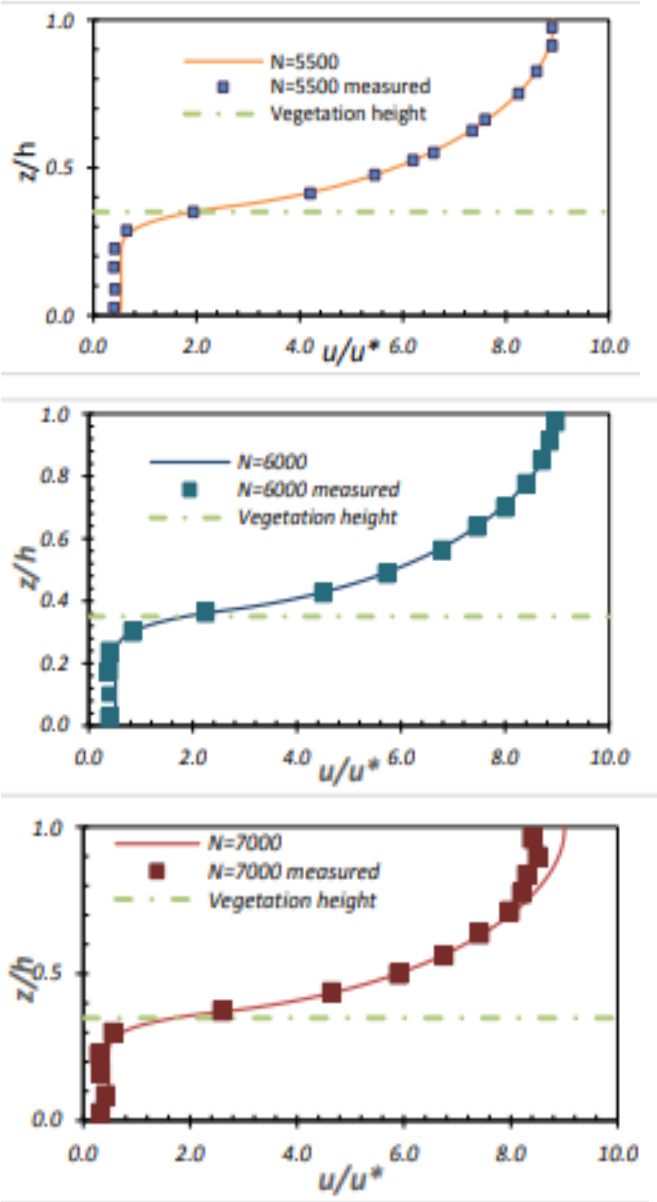

Figure 7. Mean vertical stream-wise velocity profile for very dense flexible vegetation

Reynolds shear stresses in a highly dense vegetated channel flow

In Figure 8, a good correlation exists between the experimental and modelled results. However, discrepancies arise due to low correlations of results especially in the vegetation zone arising from high-value prediction of Reynolds shear stresses. The scale of the vortex produced became minimal as the vegetation resistance balanced the gravitational flow forces.

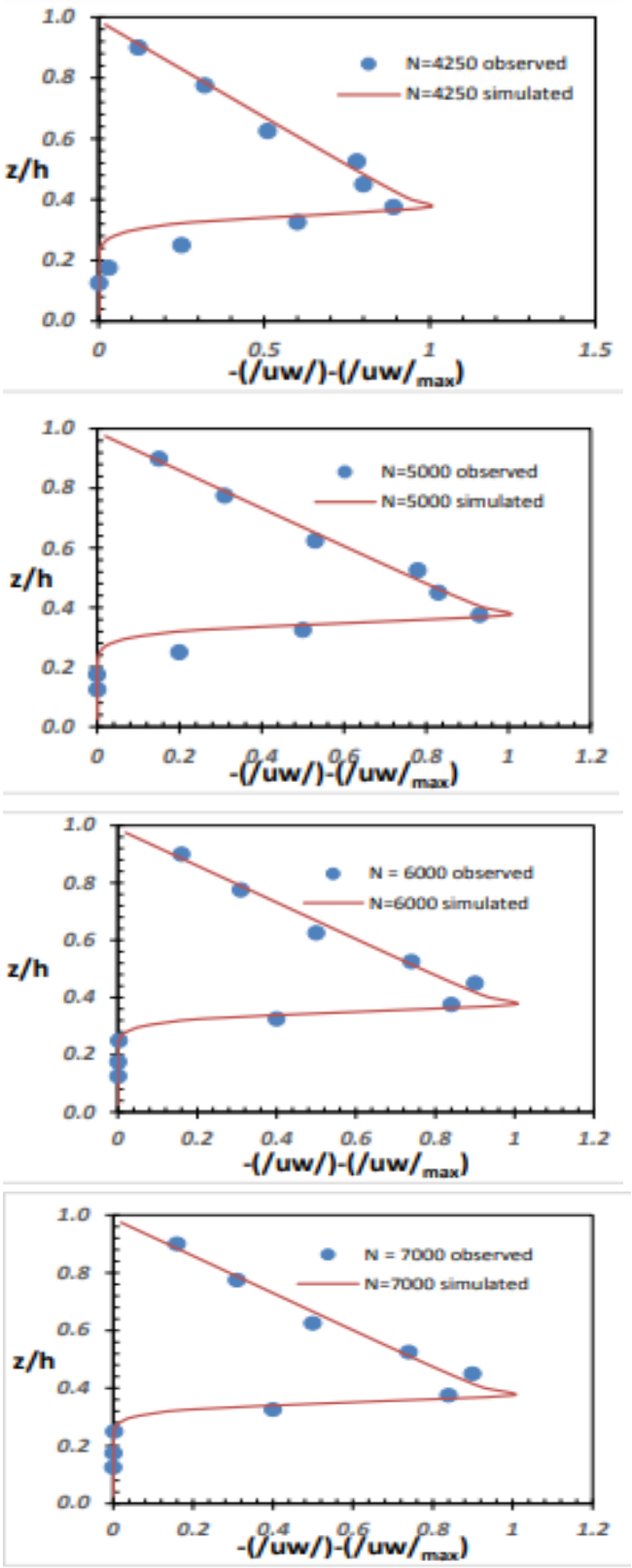

Figure 8. Measured and simulated Reynolds Shear Stresses (high density vegetation)

Re-calibration of hydraulic roughness parameters

In the case of wall-bounded shear flow, the turbulence length scale L is proportional to the distance from the point of interest to the channel bed. In the presence of varying vegetation sizes, the turbulence length scale is reduced to allow turbulence eddies above the vegetation zone to reach the channel bed. A zero-plane displacement parameter, Z_o is introduced to simulate the reduction in the turbulence length scale The L value of a point at level Z is obtained by (Eqn. 13)

$$\begin{cases} L = Z - Z_o, & Z > k_d > Z_o \\ L = Z\,(k_d - Z_o)/k_d\,, & Z < k_d \end{cases} \quad (13)$$

where k_d is the deflected height of vegetation (m).

This study adopted the empirical equation of $Z_o$developed by (Busari and Li, 2016) which is given by (Eqn. 13):

$$\frac{Z_o}{k_d} = \frac{f_v^{\beta}}{f_v^{\beta} + \alpha^{\beta}} \quad (14)$$

These roughness parameter indices are given as $\alpha = 0.7$ *and* β*=0.5*. For very high density as presented in this work, there is need to recalibrate these indices to fit the reduction in turbulent length scale required for highly dense vegetation. The parameters were varied within a suitable range until the modeled velocity profile matched the experimentally observed profile. Based on this, the best results is obtained for $\alpha = 0.56$ *and* β*=0.64*.

Modified vertical mean stream-wise velocity profile using the calibrated α and β

The velocity profiles are reproduced using the modified values of α and β in the (Eqn.14) to obtain a new $Z_o$value which is then fed into the numerical input file. The newly obtained mean vertical stream-wise velocities are shown in Figure 9.

Relationship between Maximum Reynolds Shear Stress and Vegetal Densities

In Figure 10, the fitting of the relationship between the maximum Reynolds Shear Stresses and the vegetation density shows a non-linearity properties of power law for low vegetal covers.

In Figure 11, the fitting of the relationship between the maximum Reynolds Shear Stresses and the vegetation density shows perfect linearity properties for medium vegetal covers.

In Figure 12, the fitting of the relationship between the maximum Reynolds Shear Stresses and the vegetation density shows perfect linearity properties for highly dense vegetation as observed in Figure 8. This implies that the deflection of vegetation at high densities is lowered as the vegetal density increases, due to increase in the hydraulic resistance to the flow. Hence, more water will be diverted above the vegetation zone.

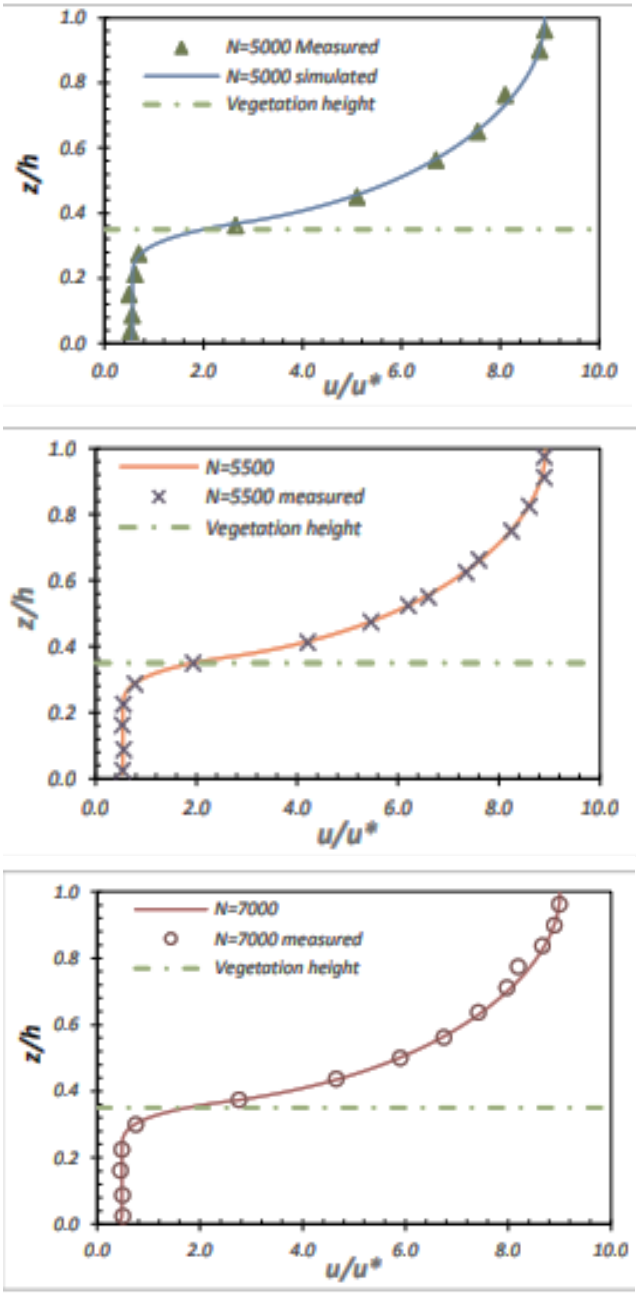

Figure 9. Mean vertical stream-wise vel. profile for dense flexible vegetation (α = 0.56 and *and* β=0.64)

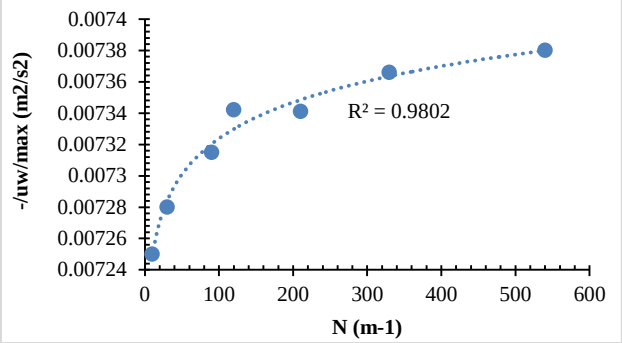

Figure 10. Maximum Reynolds Shear Stresses and vegetation density (Class I)

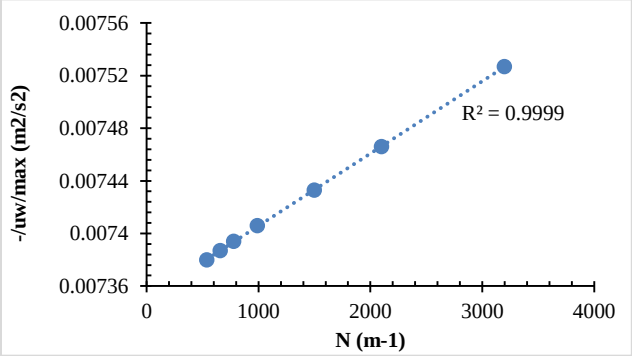

Figure 11. Maximum Reynolds Shear Stresses and vegetation density (Class II)

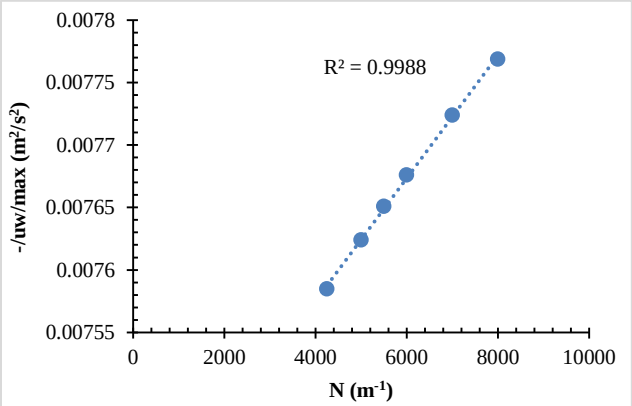

Figure 12. Maximum Reynolds Shear Stresses and vegetation density (Class III)

CONCLUSIONS

The present study deepens the understanding of vegetated channel modeling by taking into consideration the influence of zero-plane displacement parameter and the effect of varying vegetation density on the vertical mean stream-wise velocity profile of submerged flexible vegetation through the numerical simulation of laboratory flume experiments of vegetative open channel flow. The study verifies the dependency of the shapes of the vertical mean stream-wise velocity profile on the vegetal areal densities; in addition, the model replicate the vertical mean stream-wise velocity profile and Reynolds shear stress profile for varying vegetal areal densities. However, discrepancy was found in the prediction for very high density. Based on the recalibration of hydraulic roughness parameters, the 1-D RANS model replicate the vertical mean stream-wise velocity profile and Reynolds Shear Stresses accurately.

DECLARATIONS

Corresponding author

Correspondence and requests for materials should be addressed to Busari Afis; E-mail: abusari@unam.na; ORCID: 0000-0002-5737-8384

Data availability

The datasets used and/or analyzed during the current study available from the corresponding author on reasonable request.

Author's contribution

J. Kelvin participated in the design of study and ran the simulation; A.O. Busari is responsible for the conceptualization, methodology, analysis and overall discussion of modelled results and finally the review and editing of manuscript.

Acknowledgements

The author thanks the University of Namibia for funding the dissemination of output of this research.

Competing interests

The authors declare no competing interests in this research and publication.

REFERENCES

Abdullahi N, Busari AO (2021). Modeling of Open Channel Flow: A review. Iconic Research and Engineering Journals. Volume 4, Issue 9. 18-33. View article (google.com)

Abdullahi N, Busari, A. O (2021). Experimental study on the effect of River Bank vegetation in open channel flow. Proceedings of the 6th Hybrid conference of Nigerian Institution of Mechanical Engineers, Minna, Nigeria page 59-68. Google Scholar

Azorji C, Busari, AO (2021). The effect of vegetation density on flow characteristics in submerged vegetation. Proceedings of the 6th Hybrid conference of Nigerian Institution of Engineers, Minna, Nigeria. 98-106. Google Scholar

Busari AO, Li CW (2016). Bulk drag in a regular array of emergent vegetation stems under gradually varied flow. Journal of Hydro-environmental Research, volume 12, 59–69. https://doi.org/10.1016/J.JHER.2016.02.003

Chiaradia EA., Gandolfi C, Bischetti GB (2019). Flow resistance of partially flexible vegetation: A full-scale study with natural plants. Journal of Agricultural Engineering, 50, 55–65. https://doi.org/10.4081/jae.2019.885

Di Stefano C, Nicosia A, Palmeri V, Pampalone V, Ferro V (2022). Rill flow velocity and resistance law: A review. Earth-Science Reviews, 231. https://doi.org/10.1016/j.earscirev.2022.104092

Errico A, Lama GFC, Francalanci S, Chirico GB, Solari L, Preti, F (2019). Flow dynamics and turbulence patterns in a drainage channel colonized by common reed under different scenarios of vegetation management. Ecological Engineering, 133, 39–52. https://doi.org/10.1016/j.ecoleng.2019.04.016

Ferro V, Porto P (2018). Applying hypothesis of self-similarity for flow resistance law in Calabrian gravel bed rivers (Fiumare). Journal of Hydraulic Engineering, 144, 1–11. https://doi.org/10.1061/(ASCE)HY.19437900.0001385

Li CW, Busari AO (2019). Hybrid modeling of flows over submerged prismatic vegetation with different areal densities. Journal Engineering Applications of Computational Fluid Mechanics 13(1), 493-505. https://doi.org/10.1080/19942060.2019.1610501

Manko A, Busari AO (2020). Estimation of vegetative hydraulic resistance in an open channel flow. Presented at the 18th International Conference of Nigerian Institution of Civil Engineers (NICE), Abuja, Nigeria. View article (google.com)

Spalart PR, Allmaras SR (1994). A one-equation turbulence model for aerodynamic flows. La Recherche Aerospatiale, volume 1, number 1, pp 5-21. https://doi.org/10.2514/6.1992-439

Sulaimon M, Busari AO (2019). Hydraulic modeling of nature-based approach to submerged flexible Vegetation lining. International Conference of Engineering and Environmental Sciences (ICEES), Osun State University, Nigeria (Nov. 5-7, 2019). View article (google.com)

Truong SH, Uijttewaal WSJ (2019). Transverse momentum exchange induced by large coherent structures in a vegetated compound channel. Journal of Water Resources Research, 55. https://doi.org/10.1029/2018WR023273